

Voltammetric Study on the Transfer of Alkali and Alkaline Earth Metal Ions at the Aqueous/Organic Interface Facilitated by Phosphine Oxides

Kaoru OGURA,[†] Sorin KIHARA,* Shigeo UMETANI, and Masakazu MATSUI
Institute for Chemical Research, Kyoto University, Uji, Kyoto 611

(Received December 17, 1992)

The transfer of alkali metal and alkaline earth metal ions (M^z) from aqueous to nitrobenzene (NB) phases, facilitated by mono-, bi-, or tridentate phosphine oxides (PO), was investigated in terms of the voltammetry for the ion transfer across the interface of two immiscible electrolyte solutions. The complex formation of M^z with PO in the vicinity of the interface and the transfer process of M^z were clarified based on an analysis of the current-potential curves, while referring to information obtained from the synergistic ion-pair extraction of $M^z(\text{ClO}_4^-)_z$ with PO. The stability constants of M^z -PO complexes in NB were evaluated based on the half-wave potentials in the ion transfer voltammograms, and were related to the properties of M^z and PO.

Both the solvent extraction^{1,2)} and voltammetry for an ion transfer across the interface of two immiscible electrolyte solutions^{3–16)} (VITIES) concern a transfer of ions between aqueous (W) and organic (O) phases. Although, the ion transfer in the solvent extraction is realized with the aid of the counter ion or chelating agents, that in VITIES is realized by applying a potential difference or current between two solutions; the transfer of the objective ion can thus be elucidated by VITIES without any influence of the counter ion. In VITIES, the transferring ion can be specified from the potential, in which the voltammogram appears, and the number of ions transferred can be determined by the current. Voltammetry also provides information concerning such reactions occurring in the vicinity of the interface.^{6–14)}

Because of the unmatched advantages of VITIES (as mentioned above) it has been applied to analyses of such solvent-extraction processes as those of metal ions (M^z) with 1,10-phenanthroline derivatives,^{8–10)} dithizone,¹¹⁾ and 4-acyl-5-pyrazolones.¹²⁾ The theoretical equations used to express voltammograms for the ion transfer facilitated by neutral ligands have also been proposed by Samec and Papoff,⁷⁾ Doe and Freiser,¹⁰⁾ Matsuda et al.,¹³⁾ and Kakiuchi and Senda.¹⁴⁾

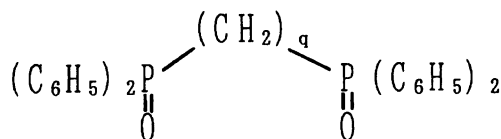
In the present paper the transfer of alkali and alkaline earth metal ions from W to nitrobenzene (NB), facilitated by the phosphine oxide derivatives (PO) given in Fig. 1, was investigated by polarography at the electrolyte solution dropping electrode,^{4,5)} which is one of the branches of VITIES. The chemical processes involved in the synergistic ion-pair extraction of M^z with PO were elucidated while referring to the polarographic results. In this regard, since PO are excellent synergistic reagents in ion-pair or chelate extractions from the view points of the strong complex formation with M^z , the low solubility in water and the weak affinity for H^+ , various derivatives, such as those given in Fig. 1, have been synthesized to obtain both improved selectivity

and extractability.^{17,18)}

Experimental

Extraction of M^z with ClO_4^- in the Presence of PO. The extraction was investigated under the following two conditions; (1) the initial concentration of PO in NB (c_{PO}^0) is much greater than the initial concentration of M^z in W (c_{M}^0). (2) c_{M}^0 is much greater than c_{PO}^0 . In an experiment under condition (1), a 10 ml aliquot of an aqueous solution (W) containing 10^{-5} M (1 M = 1 mol dm⁻³) M^z and 10^{-3} M LiClO_4 or NaClO_4 was shaken for 1 h with 10 ml of NB containing 5×10^{-5} to 10^{-2} M PO. In an experiment under condition (2), a 10 ml aliquot of W containing 1 M perchlorate salt of M^z was shaken with 10 ml of NB containing 5×10^{-5} to 10^{-2} M PO. The shaking time had been confirmed to be sufficiently long for equilibration to take place. After phase separation by centrifugation, the concentrations of M^z in W and NB were determined by an inductively-coupled argon plasma emission spectrophotometer according to the procedures mentioned previously.¹⁷⁾

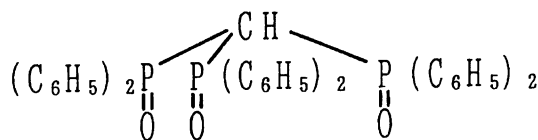
Polarographic Measurement. The current-scan



q=0: Tetraphenyldiphosphine P,P'-dioxide (TPDPDO)

q=1: Bis(diphenylphosphinyl)methane (BDPPM)

q=2: Bis(diphenylphosphinyl)ethane (BDPPE)



Tris(diphenylphosphinyl)methane (TDPPM)

Fig. 1. Phosphine oxides used in the present work.

[†]Present address: Department of Chemical and Biological Engineering, Ube Technical College, Tokiwadai, Ube 755.

polarograms were recorded using a polarographic cell reported in the previous paper.^{5,7)} The aqueous phase was dropped upward into NB through a glass capillary of an edged orifice. The apparatus (including the potentiostat, galvanostat, function generator, X-Y recorder and the device for IR drop compensation) employed were similar to those mentioned previously.^{4,5)} Crystalviolet tetraphenylborate ($\text{CV}^+\cdot\text{TPhB}^-$) was added to NB as the supporting electrolyte (SE). In an experiment under the condition that $c_{\text{PO}}^0 \gg c_{\text{M}}^0$, Na_2SO_4 was added to W as SE; in an experiment under the condition that $c_{\text{M}}^0 \gg c_{\text{PO}}^0$, the salt of M^z , served as SE.

The potential difference at the W/NB interface (ΔV) was measured using a silver/silver chloride electrode and a tetraphenylborate ion-selective electrode (TPhBE) set in W and NB, respectively. The TPhBE gave the reference potential,⁴⁾ which is the potential difference between W containing $0.025 \text{ M Mg}^{2+}\cdot(\text{TPhB}^-)_2$ and NB containing $0.05 \text{ M CV}^+\cdot\text{TPhB}^-$. The potential in the present paper refers to an imaginary potential denoted as TPhE, in which the transfer energy is equal to zero.^{4,19)} The potentials of TPhBE at 25°C referred to TPhE was 0.350 V at the W/NB interface.

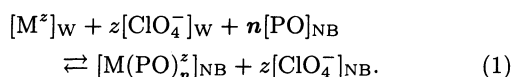
All measurements were carried out at $25 \pm 0.5^\circ\text{C}$.

Chemicals. The procedure for preparing $\text{CV}^+\cdot\text{TPhB}^-$ was identical to that mentioned previously.⁴⁾ The purification of NB was achieved by passing the solvent through a column of activated alumina. Tetraphenyldiposphine P,P' -dioxide (TPDPDO), bis(diphenylphosphinyl)methane (BDPPM), bis(diphenylphosphinyl)ethane (BDPPE), and tris(diphenylphosphinyl)methane (TDPPM) were prepared according to previously described methods.^{17,20)}

All of the other chemicals were of reagent-grade quality.

Results and Discussion

Extraction of M^z with ClO_4^- in the Presence of PO. The extraction of M^z from W containing ClO_4^- to NB in the presence of PO can be expressed as Eq. 1, since the concentrations of M^z extracted in the absence of PO were confirmed to be negligible.



Here, subscripts W and NB denote the respective phases, z the charge of M^z , and n the number of PO complexed with M^z . The ion-pair formations in both W and NB were neglected in Eq. 1 because the dielectric constants of W ($\epsilon=78.54$) and NB ($\epsilon=34.82$) were relatively large and the concentrations of $\text{M}(\text{PO})_n^z$ and ClO_4^- in NB were low.¹⁵⁾

The extraction constant (K_{ex}) for reaction (1) is given by

$$K_{\text{ex}} = [\text{M}(\text{PO})_n^z]_{\text{NB}} [\text{ClO}_4^-]_{\text{NB}}^z / [\text{M}^z]_{\text{W}} [\text{ClO}_4^-]_{\text{W}}^z [\text{PO}]_{\text{NB}}^n. \quad (2)$$

Rewriting Eq. 2, we obtain

$$\log ([\text{M}(\text{PO})_n^z]_{\text{NB}} [\text{ClO}_4^-]_{\text{NB}}^z / [\text{M}^z]_{\text{W}} [\text{ClO}_4^-]_{\text{W}}^z) = n \log [\text{PO}]_{\text{NB}} + \log K_{\text{ex}}. \quad (3)$$

The left-hand side of Eq. 3 can be obtained by substi-

tuting the concentrations of M^z determined in W and NB for $[\text{M}^z]_{\text{W}}$ and $[\text{M}(\text{PO})_n^z]_{\text{NB}}$, respectively. Here, $[\text{ClO}_4^-]_{\text{NB}}$ can be estimated from the electroneutrality: $[\text{ClO}_4^-]_{\text{NB}} = z[\text{M}(\text{PO})_n^z]_{\text{NB}}$. When the initial concentration of PO in NB is much larger than that of M^z in W ($c_{\text{PO}}^0 \gg c_{\text{M}}^0$) a plot of the left-hand side of Eq. 3 vs. $\log c_{\text{PO}}^0$ gives a straight line with a slope of n and an intercept of $\log K_{\text{ex}}$, since $[\text{PO}]_{\text{NB}}$ can be approximated by c_{PO}^0 . Under the condition that $c_{\text{M}}^0 \gg c_{\text{PO}}^0$, the plot on the left hand side of Eq. 3 vs. $\log \{c_{\text{PO}}^0 - n[\text{M}(\text{PO})_n^z]_{\text{NB}}\}$ gives a straight line with a slope of n and an intercept of $\log K_{\text{ex}}$, since $[\text{PO}]_{\text{NB}}$ is equal to $\{c_{\text{PO}}^0 - n[\text{M}(\text{PO})_n^z]_{\text{NB}}\}$.

Table 1 summarizes the n obtained from the slopes. When $c_{\text{PO}}^0 (=5 \times 10^{-5} - 10^{-2} \text{ M}) \gg c_{\text{M}}^0 (=10^{-5} \text{ M})$, the n for alkaline earth metal ions (M^{2+}) with bidentate BDPPM or BDPPE increased with an increase in the ionic radii (r) of M^{2+} . Although the n for Ca^{2+} and Sr^{2+} with bidentate BDPPM were identical with those with BDPPE, $\log K_{\text{ex}}$ for these ions in the extraction with BDPPM were larger than those with BDPPE. By employing tridentate TDPPM, the n ($=2$) were independent of M^z , and $\log K_{\text{ex}}$ for M^{2+} increased with an increase in r .

Under the condition that $c_{\text{M}}^0 (=1 \text{ M}) \gg c_{\text{PO}}^0 (=5 \times 10^{-5} - 10^{-2} \text{ M})$, the n of M^{2+} with BDPPM or BDPPE were smaller than those under the condition that $c_{\text{PO}}^0 \gg c_{\text{M}}^0$. The n for M^{2+} with TDPPM under the condition that $c_{\text{M}}^0 \gg c_{\text{PO}}^0$ were almost identical with those for $c_{\text{PO}}^0 \gg c_{\text{M}}^0$. These results indicate that the stability constants for the complex formation reactions of $\text{M}(\text{PO})_2^z$ with another PO are not very large.

The distributions of M^{2+} into NB with TOPO or TPDPDO, and those of alkali metal ions with all of the PO investigated were too poor to determine n and $\log K_{\text{ex}}$.

Current-Potential Curves for the Facilitated Transfer of M^z . The facilitated transfer of M^z by a neutral ligand (L) in O has been understood through EC and CE mechanisms^{7,10)} (cf. Fig. 2). Here, the EC mechanism indicates an ion transfer from W to O, which

Table 1. Extraction Parameters for $\text{M}(\text{PO})_n^z$

$(c_{\text{M}}^0)^{\text{a)}}$ mol dm ⁻³		PO ^{b)} in NB		Mg^{2+}	Ca^{2+}	Sr^{2+}	Ba^{2+}
10^{-5}	BDPPM	$\log K_{\text{ex}}$		4.8	7.7	6.3	8.9
		n		3.0	3.0	4.0	5.0
		BDPPE	$\log K_{\text{ex}}$		4.4	-0.6	
	TDPPM	n			3.0	4.0	
		$\log K_{\text{ex}}$		2.8	3.0	3.1	3.3
		n		2.0	2.0	2.0	2.0
1	BDPPM	n		2.0	2.0	2.1	1.9
		BDPPE	n		2.2		
		TDPPM	n	1.8	1.9	1.9	1.7

a) Initial concentration of M^z in aqueous phase.

b) Concentration of phosphine oxide, PO, in nitrobenzene: $5 \times 10^{-5} - 10^{-2} \text{ M}$.

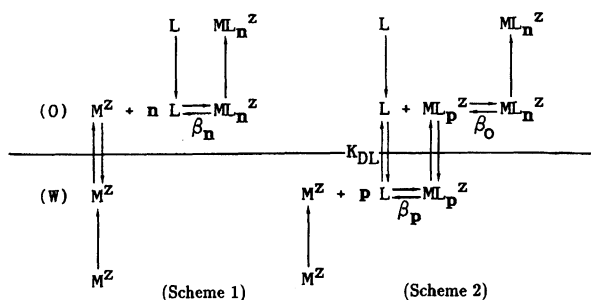


Fig. 2. Mechanisms for the transfer of a metal ion (M^z) at the aqueous/organic (W/O) interface facilitated by a neutral ligand (L).

is an electrochemical reaction (E), followed by the complex formation of M^z with L in O, which is a chemical reaction (C) (Scheme 1). The CE mechanism involves a complex formation of M^z with L distributed to W (C), followed by the transfer of an M^z -L complex from W to O (E) (Scheme 2). The transferred species (ML_p^z) may be complexed further with L, yielding ML_n^z .

Regarding Fig. 2, the constants for complex formations of M^z or ML_p^z with L and for the distribution of L occurring at the W/O interface can be defined as follows:

$$\beta_n = [ML_n^z]_O^* / [M^z]_O^* ([L]_O^*)^n, \quad (4)$$

$$\beta_p = [ML_p^z]_W^* / [M^z]_W^* ([L]_W^*)^p, \quad (5)$$

$$\beta_o = [ML_n^z]_O^* / [ML_p^z]_O^* ([L]_O^*)^{(n-p)}, \quad (6)$$

and

$$K_{DL} = [L]_O^* / [L]_W^*, \quad (7)$$

where the superscript (*) indicates the concentrations in the vicinity of the interface.

Considering that the transferring ions across the W/O interface in EC and CE mechanisms are M^z and ML_p^z , respectively, the potential difference at the W/O interface (ΔV) can be expressed as Eqs. 8 and 9, based on the Nernst equation:

(EC mechanism)

$$\Delta V = \Delta \varphi_M^0 + (RT/zF) \ln ([M^z]_O^* / [M^z]_W^*), \quad (8)$$

(CE mechanism)

$$\Delta V = \Delta \varphi_{ML_p}^0 + (RT/zF) \ln ([ML_p^z]_O^* / [ML_p^z]_W^*). \quad (9)$$

Here, $\Delta \varphi_M^0$ and $\Delta \varphi_{ML_p}^0$ are the standard Galvani potential difference for the transfer of M^z and ML_p^z , respectively, and R , T , and F have their usual meanings.

Equations 8 and 9 can be rewritten as Eqs. 10 and 11, respectively, using Eqs. 4 to 7:

$$\Delta V = \Delta \varphi_M^0 + (RT/zF) \ln ([ML_n^z]_O^* / [M^z]_W^* [L]_O^* \beta_n) \quad (10)$$

and

$$\Delta V = \Delta \varphi_{ML_p}^0 + (RT/zF) \ln ([ML_n^z]_O^* K_{DL}^p / [M^z]_W^* ([L]_O^*)^n \beta_p \beta_o). \quad (11)$$

An equation which can express the current-potential curve (polarographic wave in the present case) for the transfer of M^z facilitated by L in O has been investigated based on Eqs. 10 and 11 by several authors^{7,10,13,16)} under the assumption of a reversible transfer in which the rates of the ion transfer and the complex formation are fast and, hence, the transfer process is controlled by the diffusion of objective species. This assumption seems to be reasonable, since most of ion-transfer reactions reported so far are reversible.⁴⁻⁷⁾

Matsuda et al.¹³⁾ derived general, but rather complicated, equations for current-potential curves applicable to both the EC and CE mechanisms. Simplified equations have also proposed as follows under the assumption that the ion transfer reaction proceeds dominantly by either the EC or the CE mechanism.

(A) Current-Potential Curve Based on the EC Mechanism under the Condition That $c_L^0 \gg c_M^0$. The following equation for the curve was derived¹⁶⁾ as Eq. 12 by considering that the transfer of M^z is controlled by the diffusion of M^z in W because of the condition of $c_L^0 \gg c_M^0$:

$$\begin{aligned} \Delta V = \Delta \varphi_M^0 &+ (RT/zF) \ln \{1/\beta_n (c_L^0)^n\} \\ &+ (RT/zF) \ln (D_M/D_{ML_n})^{1/2} \\ &+ (RT/zF) \ln (\gamma_{\pm,O}/\gamma_{\pm,W}) \\ &+ (RT/zF) \ln \{I/(I_L - I)\}, \end{aligned} \quad (12)$$

where D_M and D_{ML_n} are the diffusion coefficients of M^z in W and ML_n^z in O; $\gamma_{\pm,\alpha}$ is the mean activity coefficient of a salt in α phase, I the instantaneous current and I_L the limiting current. The activity coefficient of neutral L was taken as unity.

By defining the half-wave potential ($\Delta V_{1/2}$) as ΔV at $I = I_L/2$,

$$\begin{aligned} \Delta V_{1/2} = \Delta \varphi_M^0 &+ (RT/zF) \ln (1/\beta_n) \\ &+ (RT/zF) \ln (D_M/D_{ML_n})^{1/2} \\ &+ (RT/zF) \ln (\gamma_{\pm,O}/\gamma_{\pm,W}) \\ &- n(RT/zF) \ln c_L^0. \end{aligned} \quad (13)$$

(B) Current-Potential Curve Based on the EC Mechanism under the Condition That $c_M^0 \gg c_L^0$. Samec and Papoff⁷⁾ proposed the following equation in which the transfer reaction is controlled by the diffusion of L in O:

$$\begin{aligned} \Delta V = \Delta \varphi_M^0 &+ (RT/zF) \ln (1/\beta_n c_M^0) \\ &+ (RT/zF) \ln (S_L^n/S_{ML_n}) \\ &+ (RT/zF) \ln (\gamma_{\pm,O}/\gamma_{\pm,W}) \\ &+ (RT/zF) \ln \{I/(I_L - I)^n\}, \end{aligned} \quad (14)$$

with

$$S_L = KF(z/n) D_L^{1/2} m_v^{2/3} t_d^{1/6} \quad (15)$$

and

$$S_{MLn} = KF(z/n)D_{MLn}^{1/2}m_v^{2/3}t_d^{1/6}. \quad (16)$$

Here, K is the Ilkovič constant, D_L the diffusion coefficient of L in O, m_v the mean flow rate, and t_d the drop time of W.

Further,

$$\begin{aligned} \Delta V_{1/2} = & \Delta\varphi_M^0 + (RT/zF) \ln(1/\beta_n c_M^0) \\ & + (RT/zF) \ln(D_{MLn}/D_L)^{1/2} \\ & + (RT/zF) \ln(\gamma_{\pm,O}/\gamma_{\pm,W}) \\ & - (n-1)(RT/zF) \ln(c_L^0/2). \end{aligned} \quad (17)$$

(C) Current-Potential Curve Based on the CE Mechanism under the Condition That $c_L^0 \gg c_M^0$. No equation under this condition has been proposed. By referring to the procedure used to derive Eq. 12, and considering that the transfer is controlled by the diffusion of M^z in W, the following current-potential curve under the condition that $c_L^0 \gg c_M^0$ can be derived from Eq. 11:

$$\begin{aligned} \Delta V = & \Delta\varphi_{MLp}^0 + (RT/zF) \ln\{K_{DL}^p/\beta_p\beta_o(c_L^0)^n\} \\ & + (RT/zF) \ln(D_M/D_{MLn})^{1/2} \\ & + (RT/zF) \ln(\gamma_{\pm,O}/\gamma_{\pm,W}) \\ & + (RT/zF) \ln\{I/(I_L - I)\}. \end{aligned} \quad (18)$$

Here,

$$\begin{aligned} \Delta V_{1/2} = & \Delta\varphi_{MLp}^0 + (RT/zF) \ln(K_{DL}^p/\beta_p\beta_o) \\ & + (RT/zF) \ln(D_M/D_{MLn})^{1/2} \\ & + (RT/zF) \ln(\gamma_{\pm,O}/\gamma_{\pm,W}) \\ & - n(RT/zF) \ln c_L^0. \end{aligned} \quad (19)$$

(D) Current-Potential Curve Based on the CE Mechanism under the Condition That $c_M^0 \gg c_L^0$. Doe and Freiser¹⁰ derived the following equation assuming the CE mechanism and a transfer process controlled by the diffusion of L in O:

$$\begin{aligned} \Delta V = & \Delta\varphi_{MLp}^0 + (RT/zF) \ln(K_{DL}^p/\beta_p\beta_o c_M^0) \\ & + (RT/zF) \ln(S_L^n/S_{MLn}) + (RT/zF) \ln(\gamma_{\pm,O}/\gamma_{\pm,W}) \\ & + (RT/zF) \ln\{I/(I_L - I)^n\}. \end{aligned} \quad (20)$$

Here,

$$\begin{aligned} \Delta V_{1/2} = & \Delta\varphi_{MLp}^0 + (RT/zF) \ln(K_{DL}^p/\beta_p\beta_o c_M^0) \\ & + (RT/zF) \ln(D_{MLn}/D_L)^{1/2} \\ & + (RT/zF) \ln(\gamma_{\pm,O}/\gamma_{\pm,W}) \\ & + (n-1)(RT/zF) \ln(c_L^0/2). \end{aligned} \quad (21)$$

In Eqs. 12, 13, 14, 17, 18, 19, 20, and 21, ion-pair formation is neglected, since the dielectric constants of W and NB are large and the concentration of ions in NB are low.¹⁵⁾

The I_L for reversible ion-transfer polarograms under the condition that $c_L^0 \gg c_M^0$ and $c_M^0 \gg c_L^0$ can be expressed as follows based on the Ilkovič equation:

$$I_L = KzFD_M^{1/2}m_v^{2/3}t_d^{1/6}c_M \quad (c_L^0 \gg c_M^0) \quad (22)$$

and

$$I_L = KzFD_L^{1/2}m_v^{2/3}t_d^{1/6}c_L/n \quad (c_M^0 \gg c_L^0). \quad (23)$$

Reviewing the above-mentioned equations for the current-potential curves and $\Delta V_{1/2}$ for transfers of M^z under various conditions, we notice the following: (1) The plots of $\Delta V_{1/2}$ vs. $\log c_L^0$ give straight lines with slopes of $59.2n/z$ or $59.2(n-1)/z$ mV under the condition that $c_L^0 \gg c_M^0$ or $c_M^0 \gg c_L^0$, respectively, both in the EC and CE mechanisms. (2) Logarithmic analyses of the polarograms give straight lines with slopes of $59.2/z$ mV, irrespective of n under the condition that $c_L^0 \gg c_M^0$ or $c_M^0 \gg c_L^0$ with $n=1$. When $c_M^0 \gg c_L^0$ and $n>1$, however, the logarithmic analyses of the polarograms in both EC and CE mechanisms do not give straight lines, and the polarograms vary depending on n . The shapes of the polarograms in both the EC and CE mechanisms are identical. (3) If we assume the transfer mechanism to be EC, the overall stability constant β_n in O can be evaluated from $\Delta V_{1/2}$ using $\Delta\varphi_M^0$, since $\Delta\varphi_M^0$ for many M^z have been reported. If the transfer proceeds by CE mechanism, however, it is very difficult to obtain informations concerning complex formations in W or O, since $\Delta\varphi_{MLp}^0$ are hard to estimate.

Polarogram for the Transfer of M^z at the W/NB Interface under the Condition That $c_{PO}^0 \gg c_M^0$. Curve 1 in Fig. 3 illustrates the residual polarogram at the interface of W containing 0.05 M Na_2SO_4 and NB containing 0.05 M $\text{CV}^+\cdot\text{TPhB}^-$ and 10^{-2} M BDPPE. The final rise and the final descent correspond to the transfer of Na^+ from W to NB and that of CV^+ from NB to W, respectively. Polarograms 2, 3, 4, or 5 were recorded by adding 10^{-4} M of Ca^{2+} to W and 2×10^{-3} , 5×10^{-3} , 10^{-2} , or 2×10^{-2} M of BDPPE to NB, respectively. The limiting currents (I_L) were proportional to the concentration of Ca^{2+} in W over the range between 5×10^{-5} and 5×10^{-4} M and to the square root of the height of the aqueous solution reser-

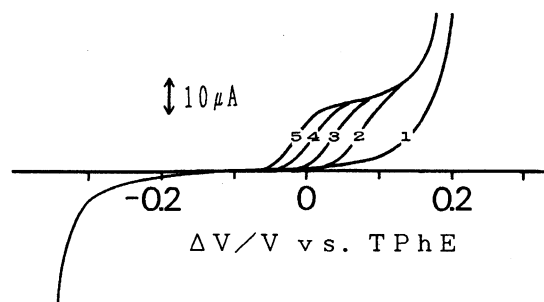


Fig. 3. Polarograms for the transfer of Ca^{2+} from an aqueous solution containing 10^{-4} M Ca^{2+} and 0.05 M Na_2SO_4 to nitrobenzene containing BDPPE and 0.05 M $\text{CV}^+\cdot\text{TPhB}^-$. Concentration of BDPPE: (1) 0, (2) 2×10^{-3} , (3) 5×10^{-3} , (4) 10^{-2} , and (5) 2×10^{-2} M.

voir, while I_L were independent of c_{BDPPE} . Logarithmic analyses of the polarograms (ΔV vs. $\log \{I/(I_L - I)\}$) based on Eq. 12 or 18 gave straight lines with slopes of 29 ± 3 mV. The characteristics of I_L and the polarographic waves suggest that the transfer of Ca^{2+} from W to NB facilitated by BDPPE is controlled by the diffusion of Ca^{2+} in W.

Although $\Delta V_{1/2}$ in polarograms 2 to 5 were independent of c_{Ca} , $\Delta V_{1/2}$ shifted by about 90 mV to become more negative when the concentration of BDPPE was increased by 1 order, i.e., $\Delta V_{1/2}$ were +0.069, +0.033, +0.008, and -0.018 V vs. TPhE when c_{BDPPE} were 2×10^{-3} , 5×10^{-3} , 10^{-2} , and 2×10^{-2} M, respectively. Hence, n in the complex $\text{Ca}(\text{BDPPE})_n^{2+}$ was estimated to be 3 according to Eq. 13 or 19. The n agrees with that obtained in solvent extraction under the condition that $c_{\text{BDPPE}}^0 \gg c_{\text{M}}^0$.

Assuming a transfer of Ca^{2+} by the EC mechanism, $\log \beta_3$ was estimated to be 18.4 based on Eq. 13. Here, the $\Delta \phi_{\text{Ca}}^0$ used was 0.354 V³⁾ vs. TPhE, and γ_{\pm} were those reported^{21,22)} for W containing 0.05 M Na_2SO_4 and NB containing 0.05 M $\text{CV}^+ \cdot \text{TPhB}^-$. The D_{Ca} in W was $6.5 \times 10^{-6} \text{ cm}^2 \text{ s}^{-1}$, obtained from I_L based on Eq. 22 and substituting I_L , m_v , t_d , and c_{Ca} . The $D_{\text{Ca}}(\text{BDPPE})_3$ was estimated to be $1.1 \times 10^{-6} \text{ cm}^2 \text{ s}^{-1}$ under an assumption described later.

Although various polarograms were examined employing Li^+ , Na^+ , Mg^{2+} , Ca^{2+} , or Sr^{2+} as M^z and BDPPM, BDPPE, or TDPPM as PO under the condition that $c_{\text{PO}}^0 \gg c_{\text{M}}^0$, well-defined waves were not observed, except for the Ca^{2+} /BDPPE system mentioned above, since the addition of PO made the potential window of the residual current narrow.

Polarogram for the Transfer of M^z at the W/NB Interface under the Condition That $c_{\text{M}}^0 \gg c_{\text{PO}}^0$. Curve 1 in Fig. 4 illustrates the residual polarogram obtained at the interface between W containing 1 M MgCl_2 and NB containing 0.05 M $\text{CV}^+ \cdot \text{TPhB}^-$ in the absence of PO. By adding 2×10^{-4} M BDPPM, BDPPE, or TDPPM into NB, the respective polarograms 2, 3, or 4 were observed. The anodic waves are attributable to the transfer of Mg^{2+} from W to NB, facilitated by PO. The I_L in polarograms 2 and 4 were proportional to the square root of the height of the water reservoir and c_{PO} in the range from 2×10^{-4} to 10^{-3} M. These results suggest that the transfer reactions involved in these polarograms are reversible, even under the condition that $c_{\text{M}}^0 \gg c_{\text{PO}}^0$.

The $\Delta V_{1/2}$ with BDPPM, BDPPE, TDPPM, TPDPO, and TOPO are summarized in Table 2. Here, the differences between $\Delta V_{1/2}$ for the transfer of Mg^{2+} from W containing 1 M MgSO_4 to NB and those from W containing 1 M MgCl_2 (about 45 mV) were attributable to the ion-pair formation of Mg^{2+} with SO_4^{2-} in W, which is not negligible (the formation constant is reported²³⁾ to be between 135 and 174). The ion-pair formations in W are negligible²⁴⁾ for all salts investi-

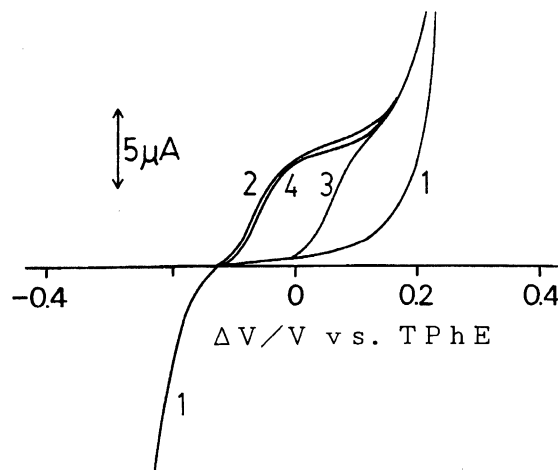


Fig. 4. Polarograms for the transfer of Mg^{2+} from an aqueous solution containing 1 M MgCl_2 to nitrobenzene, NB, containing PO and 0.05 M $\text{CV}^+ \cdot \text{TPhB}^-$. (1) residual polarogram without PO in NB. (2) 2×10^{-4} M BDPPM, (3) 2×10^{-4} M BDPPE, (4) 2×10^{-4} M TDPPM in NB.

gated in the present work, except for those comprising dication and dianion, such as MgSO_4 , when c_{salt} is 1 M.

Comparing $\Delta V_{1/2}$ at a definite c_{PO} , $\Delta V_{1/2}$ with BDPPM was 120 to 150 mV more negative than those with BDPPE, irrespective of the kind of M^z , thus indicating that BDPPM facilitates the transfer of M^z more remarkably than does BDPPE, though both BDPPM and BDPPE are bidentate ligands. The $\Delta V_{1/2}$ with tridentate TDPPM were more negative than those with bidentate BDPPM when M^{2+} were of large ionic radii, such as Sr^{2+} and Ba^{2+} . However, $\Delta V_{1/2}$ with TDPPM were less negative than those with BDPPM when M^{2+} was of small ionic radii, such as Mg^{2+} and Ca^{2+} .

The $\Delta V_{1/2}$ for the transfer of cations facilitated by PO shifted to negative linearly with an increase in $\log c_{\text{PO}}$, as shown in Table 2. Table 2 also summarizes the n obtained from the slopes of the plots of $\Delta V_{1/2}$ vs. $\log c_{\text{PO}}$ using Eq. 17 or Eq. 21.

Logarithmic analyses of polarograms 2, 3, and 4 in Fig. 4 did not give straight lines. Curves 1, 2, and 3 in Fig. 5 are current-potential curves for the transfer of M^{2+} from W to O containing 2×10^{-4} M PO, which were calculated according to Eq. 14 or Eq. 20, and assuming n as being 1, 2, and 3, respectively. The $\Delta V_{1/2}$ employed in the calculation was that -0.072 V vs. TPhE, which was observed with the Mg^{2+} /BDPPM system. The curve calculated adopting $n=2$ agrees fairly well with the polarogram observed for the Mg^{2+} /BDPPM system (curve 2 in Fig. 4), which is replotted as curve 4 in Fig. 4. Other polarograms, the $\Delta V_{1/2}$ of which are listed in Table 2, with standard deviations of 3 mV were also confirmed to be reproducible by the simulated current-potential curves with the n given in Table 2. The agreement between current-potential curves

Table 2. Half-Wave Potentials^{a)} for the Transfer of Cations, M^z , from Aqueous^{b)} to Nitrobenzene, NB, Facilitated by Phosphine Oxides, PO

M ^z	PO in NB	Concentration of PO in NB/mol dm ⁻³						n
		10 ⁻⁴	2×10 ⁻⁴	5×10 ⁻⁴	10 ⁻³	2×10 ⁻³	5×10 ⁻³	
Mg ²⁺ (Cl ⁻) ^{c)}	BDPPM		-72(3) ^{d)}	-80(3)	-91(3)			1.9
Mg ²⁺ (SO ₄ ²⁻)		-15(3)	-23(3)	-35(3)				2.0
Ca ²⁺ (Cl ⁻)		-155(3)	-162(3)	-175(3)				2.0
Sr ²⁺ (Cl ⁻)		-32(3)	-43(3)	-57(3)	-68(3)			2.1
Ba ²⁺ (Cl ⁻)		-40(3)	-49(3)	-61(3)	-76(3)			2.2
Li ⁺ (SO ₄ ²⁻)				-5(3)	-11(3)	-16(3)		1.3
Na ⁺ (SO ₄ ²⁻)				93(5)	82(5)	73(5)		1.6
K ⁺ (SO ₄ ²⁻)				40(10)	34(10)			1.3
Rb ⁺ (SO ₄ ²⁻)				20(10)	10(10)	4(10)		1.4
Cs ⁺ (SO ₄ ²⁻)				40(10)	30(10)	20(10)		1.6
H ⁺ (SO ₄ ²⁻)				75(10)				
Mg ²⁺ (Cl ⁻)	BDPPE	68(5)	52(5)	40(5)	25(5)			2.4
Mg ²⁺ (SO ₄ ²⁻)		113(10)	98(5)	80(5)	65(5)			2.6
Ca ²⁺ (Cl ⁻)		-12(3)	-25(3)	-34(3)	-40(3)	-55(3)		2.0
Sr ²⁺ (Cl ⁻)			90(5)	77(5)	55(5)	47(5)		2.5
Ba ²⁺ (Cl ⁻)				120(10)	111(10)	100(10)		2.1
Li ⁺ (SO ₄ ²⁻)				123(10)	119(10)	115(10)	111(10)	1.2
Mg ²⁺ (Cl ⁻)	TDPPM	-50(3)	-58(3)	-67(3)				1.9
Mg ²⁺ (SO ₄ ²⁻)		-10(3)	-19(3)	-29(3)				1.9
Ca ²⁺ (Cl ⁻)		-54(3)	-64(3)	-75(3)				2.0
Sr ²⁺ (Cl ⁻)		-67(3)	-76(3)	-87(3)				2.0
Ba ²⁺ (Cl ⁻)		-89(3)	-97(3)	-103(3)				1.7
Li ⁺ (SO ₄ ²⁻)		59(5)	58(5)	57(5)	52(5)	53(5)	54(5)	1.1
Na ⁺ (SO ₄ ²⁻)				-25(5)	-15(5)			1.6
Mg ²⁺ (Cl ⁻)	TPDPDO				>250(10)			
Ca ²⁺ (Cl ⁻)						250(10)		
Ba ²⁺ (Cl ⁻)						210(10)		
Mg ²⁺ (SO ₄ ²⁻)	TOPO						213(10)	
Li ⁺ (SO ₄ ²⁻)							174(10)	

a) mV vs. TPhE. b) Aqueous solutions contain 1 M salt of M^z . c) Anions in the parentheses are counter ions in the salts. d) Standard deviation in the measurements of $\Delta V_{1/2}$.

observed and those calculated supports the results described previously, that transfer processes of M^z from W to NB in the presence of PO under $c_M^0 \gg c_{PO}^0$ are reversible, indicating that the n given in Table 2 are reasonable.

M^z -PO Complexes in the Vicinity of the Interface and in the Bulk of NB. The ΔV in the polarographic measurement is determined by the ionic species and its concentration in the vicinity of the W/NB interface, though K_{ex} in solvent extraction is determined by those in bulks of W and NB after the equilibrium. In the present work, the n obtained from $\Delta V_{1/2}$ were confirmed to be nearly equal to those from K_{ex} under both the following conditions: $c_{PO}^0 \gg c_M^0$ and $c_M^0 \gg c_{PO}^0$. This suggests that the species existing in the vicinity of the interface immediately after a transfer to NB are the same as those in the bulk of NB after equilibrium, as long as M^z are alkali metal or alkaline earth metal ions and the neutral ligands are PO.

Relation between $\Delta V_{1/2}$ and $\log K_{ex}$. It is difficult to discuss the relation based on $\log K_{ex}$ and $\Delta V_{1/2}$ obtained under the same condition for c_M^0 and c_{PO}^0 , since these constants (observed under such a condition) were limited to those for Ca^{2+} with BDPPE under the condition that $c_{BDPPE}^0 \gg c_M^0$ in the present work. Hence, as the second-best choice, the $\log K_{ex}$ obtained with TDPPM under $c_{TDPPM}^0 \gg c_M^0$ were compared with $\Delta V_{1/2}$ with TDPPM under the condition that $c_M^0 \gg c_{TDPPM}^0$, while taking into account that the M^{2+} -TDPPM complex formed in NB under both $c_{TDPPM}^0 \gg c_M^0$ and $c_M^0 \gg c_{TDPPM}^0$ conditions are the same, $[M(TDPPM)_2]^{2+}$.

A linear relation was found between $\log K_{ex}$ and $\Delta V_{1/2}$, as plotted in Fig. 6, suggesting that the estimation of $\log K_{ex}$ or $\Delta V_{1/2}$ would be possible from $\Delta V_{1/2}$ or $\log K_{ex}$, respectively, though a further consideration is required.

Complex Formation of M^z with PO in NB. As

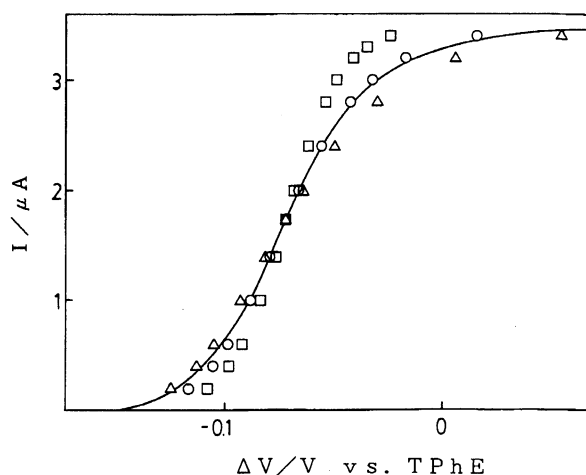


Fig. 5. Current-potential curves simulated based on Eq. 14 or 20 for the transfer of M^{2+} facilitated by BDPPM. Curves 1 (\square), 2 (\circ), and 3 (\triangle): calculated assuming n in $Mg(BDPPM)_n^{2+}$ as 1, 2, and 3, respectively. Curve 4 (—): the curve observed.

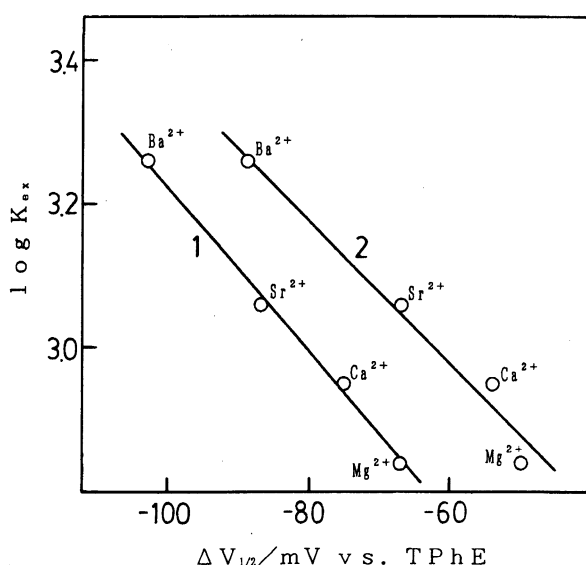


Fig. 6. Relation between $\log K_{ex}$ for M^{2+} obtained with TDPPM under the condition of c_{TDPPM}^0 (5×10^{-5} – 10^{-2} M) $\gg c_M^0$ (10^{-5} M) and $\Delta V_{1/2}$ for the transfer of M^{2+} facilitated by TDPPM under $c_M^0(1M) \gg c_{TDPPM}^0$. c_{TDPPM}^0 in the measurement of $\Delta V_{1/2}$: (1) 5×10^{-4} , (2) 10^{-4} M.

mentioned previously, β_n can be evaluated from polarographic data using the reported $\Delta\varphi_M^0$ if we assume the transfer process is by the EC mechanism.

The $\log \beta_n$ for $M(PO)_n^z$ formed in NB under the condition that $c_M^0 \gg c_{PO}^0$ were calculated based on Eq. 17, and are plotted as the function of $z^2 r^{-1}$ in Fig. 7. In the calculation, $\Delta\varphi_M^0$ from the literature³⁾ and $\Delta V_{1/2}$, n and c_{PO} in Table 2 were used (the data used for Mg^{2+} were those employing $MgCl_2$). The activity coefficients for M^z in W and $M(PO)_n^z$ in NB employed were identi-

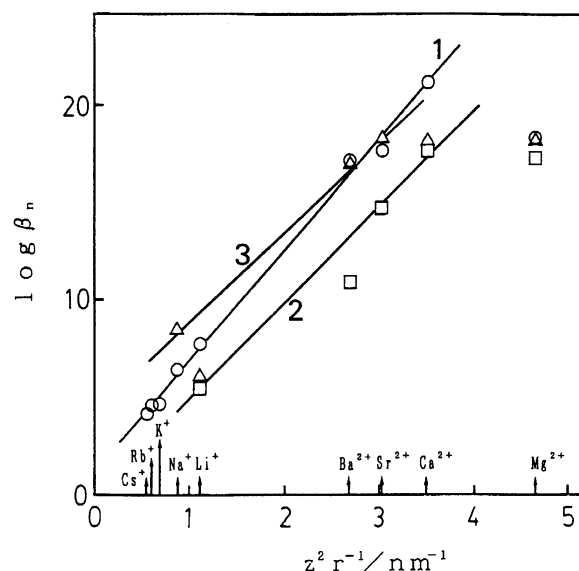


Fig. 7. Relation between $\log \beta_n$ and $z^2 r^{-1}$ for various M^z of ionic radii of r . β_n : overall stability constant of $M(PO)_n^z$ in NB. PO: curve 1 BDPPM (\circ), 2 BDPPE (\square), and 3 TDPPM (\triangle).

cal to those reported^{22,25)} for aqueous salt solutions and for NB containing 0.05 M $CV^+ \cdot TPhB^-$, respectively. The D_{BDPPM} , D_{BDPPE} , and D_{TDPPM} were evaluated to be 1.6×10^{-6} , 1.6×10^{-6} , and 1.4×10^{-6} $cm^2 s^{-1}$, respectively, from I_L , n , m_v , and t_d with the aid of Eq. 23. The $D_{M(PO)_n}$ were taken as $n^{-1/3} D_{PO}$, while assuming that $M(PO)_n^z$ are spherical and that their volumes are n -times those of PO .²⁶⁾ The ionic radii of M^z were those proposed by Shannon for 6-coordinate metal ions.²⁷⁾

The β_n is considered to be determined by the electrostatic contribution,²⁶⁾ such as a Born-type and/or ion-dipole, which depend on the z and r of M^z , and the basicity of PO and the non-electrostatic contribution, such as the chelate effect, the distance between donor oxygen atoms (which is called the "bite size"), and the steric hindrance, which depends mainly on the structure of PO .²⁸⁾

A linear relation is found between $\log \beta_n$ and $z^2 r^{-1}$ for M^z , except for Mg^{2+} , when PO is BDPPM. This relation indicates that the differences among β_n for various M^z arise mainly from the electrostatic contribution. The small $\log \beta_n$ for Mg^{2+} may be due to the small r of Mg^{2+} , compared with the "bite size" of BDPPM.

The $\log \beta_n$ obtained with BDPPE also changed almost linearly with $z^2 r^{-1}$, though the $\log \beta_n$ were smaller than those with BDPPM. The smaller $\log \beta_n$ is attributable to the larger entropy loss²⁸⁾ in the complex formation of M^z with BDPPE, which has two CH_2 between the $P=O$ groups, than that with BDPPM, which has one CH_2 between the $P=O$ groups. In this connection, smaller formation constants have been reported in the adduct formation of M^z -acylpyrazolone chelate with PO .^{17,29)}

Employing tridentate TDPPM, though $\log K_{\text{ex}}$ was expected to be larger than that with BDPPM from the view points of the chelate effect, the $\log \beta_n$ obtained for Ca^{2+} was smaller than that with BDPPM. The distance between M^z and the donor oxygen atom in the M^z -TDPPM complex is considered to be larger than that in the M^z -BDPPM complex, considering the "bite size" of TDPPM (0.351–0.413 nm) and BDPPM (0.384 nm), which had been evaluated with the aid of a PM3 calculation (UniChem MNDO90, CRAY Research Inc.). This consideration accounts for the reduced $\log \beta_n$ for M^z -TDPPM complexes, especially when M^z are of small ionic radii, such as Mg^{2+} and Ca^{2+} .

Finally, the correlation between $\log \beta_n$ and $z^2 r^{-1}$ found with BDPPM or BDPPE in the present work might be one evidence to support the assumption used in the calculation of $\log \beta_n$: that the transfer of M^z at the W/NB interface facilitated by PO proceeds by the EC mechanism.

References

- 1) Y. Marcus and A. S. Kertes, "Ion Exchange and Solvent Extraction of Metal Complexes," Wiley Interscience, London (1969).
- 2) T. Sekine and Y. Hasegawa, "Solvent Extraction Chemistry," Mcel Dekker, New York (1977).
- 3) J. Koryta, *Electrochim. Acta*, **29**, 445 (1984).
- 4) S. Kihara, M. Suzuki, K. Maeda, K. Ogura, S. Umetani, M. Matsui, and Z. Yoshida, *Anal. Chem.*, **58**, 2954 (1986).
- 5) S. Kihara, M. Suzuki, K. Maeda, K. Ogura, and M. Matsui, *J. Electroanal. Chem.*, **271**, 107 (1989).
- 6) Z. Samec, D. Homolka, and V. Marecek, *J. Electroanal. Chem.*, **135**, 265 (1982).
- 7) Z. Samec and P. Papoff, *Anal. Chem.*, **62**, 1010 (1990).
- 8) Z. Yoshida and H. Freiser, *J. Electroanal. Chem.*, **179**, 31 (1984).
- 9) Z. Yoshida and H. Freiser, *Inorg. Chem.*, **23**, 3931 (1984).
- 10) H. Doe and H. Freiser, *Anal. Sci.*, **7**, 303 (1991).
- 11) Y. Yu and H. Freiser, *Anal. Chem.*, **61**, 1621 (1989).
- 12) S. Lin and H. Freiser, *Anal. Chem.*, **59**, 2834 (1987).
- 13) H. Matsuda, Y. Yamada, K. Kanamori, Y. Kudo, and Y. Takeda, *Bull. Chem. Soc. Jpn.*, **64**, 1497 (1991).
- 14) T. Kakiuchi and M. Senda, *J. Electroanal. Chem.*, **300**, 431 (1991).
- 15) M. Suzuki, S. Kihara, K. Maeda, K. Ogura, and M. Matsui, *J. Electroanal. Chem.*, **292**, 231 (1990).
- 16) S. Kihara and Z. Yoshida, *Talanta*, **31**, 789 (1984).
- 17) S. Umetani and M. Matsui, *Anal. Chem.*, **64**, 2288 (1992).
- 18) S. Umetani, N. Shigemura, S. Kihara, and M. Matsui, *Talanta*, **38**, 653 (1991).
- 19) E. Grunwald, G. Baughman, and G. Kohnstam, *J. Am. Chem. Soc.*, **82**, 5801 (1960).
- 20) J. Chatt and F. A. Hart, *J. Chem. Soc.*, **1960**, 1378.
- 21) R. N. Goldberg, *J. Phys. Chem. Ref. Data*, **10**, 671 (1981).
- 22) S. Kihara, M. Suzuki, K. Maeda, K. Ogura, and M. Matsui, *J. Electroanal. Chem.*, **210**, 147 (1986).
- 23) E. Högfeldt, "Stability Constants of Metal-Ion Complexes Part A: Inorganic Ligands," Pergamon, Oxford (1982), p. 166.
- 24) K. Ogura, S. Kihara, M. Suzuki, and M. Matsui, *J. Electroanal. Chem.*, in press.
- 25) R. A. Robinson and R. H. Stokes, "Electrolyte Solutions," Butterworths, London, (1955).
- 26) J. O'M. Bockris and A. K. N. Reddy, "Modern Electrochemistry," Plenum Press, New York (1970), pp. 57 and 379.
- 27) R. D. Shannon, *Acta Crystallogr., Sect. A*, **32**, 751 (1976).
- 28) F. A. Cotton and G. Wilkinson, "Advanced Inorganic Chemistry," John Wiley & Sons, New York (1980), Chap. 3.
- 29) S. Umetani, S. Kihara, and M. Matsui, *Anal. Chim. Acta*, **232**, 293 (1990).